Robust polytopic LPV based Adaptive Cruise Control design for Autonomous Vehicle System

Ahmad Abubakar, Kabiru Ibrahim Dahiru, Sulaiman Haruna Sulaiman, Hamza Mustapha

Abstract— This paper studies the Adaptive Cruise Control (ACC) of longitudinal control of autonomous vehicle. The time-varying nonlinear dynamic of the longitudinal cruise control is translated into a Linear Parameter Varying (LPV) system via a Quasi-LPV approximation techniques to form a polytope, taking into consideration vehicle and road uncertainties. A dynamic state feedback controller satisfying H-infinity performance is designed at each vertex of the polytope parameter space, numerically solved using Linear Matrix Inequality (LMI) approach. With these sets of vertex controllers, a polytopic LPV controller is finally formulated. The quadratic stability of this controller is proven using Lyapunov criteria with its exponential convergence implying ride comfort. Simulation results guarantee tracking performance and robustness to variations in mass and road slope.

Index Terms—Adaptive Cruise Control, H-infinity, Linear Matrix Inequality, Polytope LPV control, Road Grade, Robust Control, Robustness.

1 INTRODUCTION

THE use of autonomous vehicles is rapidly increasing across the globe. A recent survey shows a high percentage increase in vehicle production worldwide, with 4.5% increase as up 2018 by Organisation Internationale des Constructeursd' Automobiles (OICA). This increase brings the need of optimizing the use of highway and energy resources, driving safety and comfortability and as well, traffic through-put to develop new vehicles. A lot of challenges are expected to develop vehicles that can satisfied these varied and often disagreeing requirements. To meet this challenge, automobiles industries focus on research to develop flexible, reliable and economical automotive systems. Advanced Driver Assistance Systems (ADAS) are developed to automate routine driving operation and enhancing safety and passenger comfort, Traffic flow, Energy resource etc. but at the same time the responsibility remains with the driver, to override the assistance, with prominence on improving system performance and robustness in [1].

Among the existing ADAS that performs longitudinal control of vehicle, Adaptive Cruise Control (ACC) assist the driver for speed regulation, its tracks and maintain the desired speed set by the driver, being the reference point for recent car-following applications. Its composed of classical cruise control systems with automate brake actuator and ranging sensors. This ACC system plays an important role in the safe motion of vehicles in the same lane; thus, these systems are now in focus of research and development of the automotive industry. Different control methods are used in the literature for adaptive cruise control design in order to improve its performance and robustness with respect to vehicle and road uncertainties.

Among the recent development of cruise control solutions, multi-objective optimization strategy has been proposed in [2]. In this paper, several weighting factors such as road inclination, speed limits, energy saving etc. are taken into consideration in realizing a speed profile, simulation result obtained shows a great increase in overall system energy efficiency. Subsequently, to analyze the effect vehicle and road parameter variations on the optimal speed profile, with the same optimization techniques in [2] that depend on several parameters such as Mass of the vehicle, initial conditions, height of hill etc. simulation results in [3] shows significant dependency of speed profile on parameter.

To furtherly investigate the effect of external disturbances on the system stability and speed tracking performance, an additional knowledge such as road inclinations and speed limits are taken into account for control design. Several methods have already been proposed; one is H-infinity control approach with an optimal reference speed as an uncertain dynamical system in [4]. In which simulation results shows sufficient stability and speed tracking and robust to uncertainties. Adopting the same control problem in [4], but with different control approach of state feedback H-infinity is also proposed in [5], This method is based on the assumption that information about the road is available, experimental and

- *Ahmad Abubakar is currently pursuing master's degree program in system, control and IT in University Grenoble Alpes, France, +2347038178833. ahmad.abubakar@etu.univ-grenoble-alpes.fr*
- *Kabiru Ibrahim Dahiru, dept of computer engineering, Kano state polytechnic, Nigeria, +2348036559060. kabirudahiruibrahin@kanopoly.edu.ng*
- *Sulaiman Haruna Sulaiman, dept of Electrical and electronics engineering, Ahmadu bello university, zaria, Nigeria. +2348058094931. shsulaiman@abu.edu.ng*
- *Hamza Mustapha, dept of Electrical and electronics engineering, Ahmadu bello university, Zaria, +2348106068275. hmustapha@abu.edu.ng*

simulation results guarantee its robust performance to mass variation and actuator uncertainties. Hence, we can conclude that future improvement on ACC tracking performance need more robust control to guarantee its robustness to variation of vehicle and road parameters.

Finally, in this paper, we will adopt the longitudinal model used in [5] to develop a polytopic Linear Parameter Varying (LPV) control scheme based on H-infinity strategies, that will greatly improve the speed tracking performance and guarantee its robustness to parameter variations.

2 Vehicle Oriented Control Model

2.1 Longitudinal Dynamics of Vehicle

In order to improve the cruise control of autonomous vehicles, the speed profile control is essential, which will be based on the longitudinal dynamics of a vehicle. these dynamics can be mathematically described using set of simplified non-linear differential equations (1) and (2) below [5]:

$$m\dot{v}_x = F_x - F_{aero} - R_x - mgsin\theta \quad (1)$$

$$\dot{F}_x = F_x/-\tau + u/\tau \quad (2)$$

Equation (1) represent the longitudinal on of the vehicle taking in to consideration Aerodynamics, road condition and (2) represent the first-order dynamic of the driving force actuator depending on current driving and braking condition. In the model, u is the required driving force and τ is the Actuator time constant. Now, to fully introduce the nonlinearity of the dynamics.

$$m\dot{v}_x = F_x - (1/2)\rho C_d A_f {v_x}^2 - C_r mgcos\theta - mgsin\theta \quad (3)$$

Where C_d and C_r are aerodynamics drag and rolling resistance coefficients, θ is the road slope.

Remark: the actual nonlinearity of the tire is not within the scope of this paper.

To formulate the LPV model of the system two varying parameters were considered in (4): the time varying speed v(t) and bounded mass uncertainty (i.e. up to 150% of nominal mass).

$$\rho_1 = v(t)$$
$$\rho_2 = 1/m \quad (4)$$

Assuming that the road condition (i.e. road slope θ) is a known measurable signal through ACC sensors such as GPS, lidar, Radar. The nonlinear model (3) can be approximate using quasi-LPV (q-LPV) techniques to yield the expression:

$$\dot{v}_x = -\left((1/2)\rho C_d A_f\right)\rho_1\rho_2 v_x + \rho_2 F_x - d(\theta) \quad (5)$$

Where $\rho_1 \in [\rho_{1min}, \rho_{1max}]$ is the bounded speed parameter and $\rho_2 \in [\rho_{2min}, \rho_{2max}]$ is the bounded mass variation of the vehicle and $d(\theta)$ is measured disturbance, which represent sum of tire and inclination resistance.

Working with higher values of dependent parameters (e.g. Mass of 1200kg) is in-convenient, we normalize each parameter dependent to be $\rho \leq 1$ as in (6).

$$\hat{\rho}_1 = \rho_1/\rho_{1max}$$
$$\hat{\rho}_2 = \rho_2/\rho_{2max} \quad (6)$$

Now the LPV model becomes:

$$\dot{v}_x = -\left(1/2\,\rho C_d A_f\right)\rho_{1max}\rho_{2max}\widehat{\rho_1}\widehat{\rho_2}v_x + \rho_{2max}\widehat{\rho_2}F_x - d(\theta) \quad (7)$$

The state representation of the LPV longitudinal dynamics can now be described in the following way:

$$\dot{x} = \mathrm{A}(\rho)x + \mathrm{B}u + d(\theta)$$
$$y = Cx \quad (8)$$

Where:

$$\dot{x} = \begin{bmatrix}\dot{v}_x \\ \dot{F}_x\end{bmatrix} \text{ and } x = \begin{bmatrix}v_x \\ F_x\end{bmatrix}$$

$$A = \begin{bmatrix} -\left(\frac{1}{2}\rho C_d A_f\right)\rho_{1max}\rho_{2max}\widehat{\rho_1}\widehat{\rho_2} & \rho_{2max}\widehat{\rho_2} \\ 0 & \frac{1}{-\tau} \end{bmatrix}, B = \begin{bmatrix}0 \\ \frac{1}{\tau}\end{bmatrix}$$

Thus, the realized engine force F_x is designed from the control input u through the drive actuator to handle the parameter variations and measured disturbances d.

2.2 Polytopic LPV representation

The state matrix $A(\rho)$ of the LPV model (8) is a function of the varying parameters and also affinely dependent. Thus, we can used "Polytopic model" for synthesis and analysis. The vector of parameters evolves inside a polytope represented by ω_i= 2^Nnumber of vertices of the polytope formed by the extremum values of each varying parameter.

With 2 dependent parameters ρ_1 *and* ρ_2, we have 4 number of Vertices, the state matrix $A(\rho)$ is described by (9).

$$A(\rho) = \sum_{i=1}^{N} \alpha_i(\rho)A(\omega_i) \quad (9)$$

The polytopic model representation is fully describe in the following way:

$$\Sigma(\rho) = \sum_{i=1}^{N} \alpha_i(\rho)\begin{bmatrix}A(\omega_i) & B \\ C & D\end{bmatrix} \quad (10)$$

Which is subjected to convex combination: $\sum_{i=1}^{2^N} \alpha_i(\rho) = 1$ *and* $\alpha_i(\rho) > 0$

Testing the individual stability of each vertex of the polytope may not guaranty the stability of the system at all operating point, thus, to test the global stability (i.e. Quadratic stability) at all operating condition, one can numerically solved Linear Matrix Inequality (LMI) constraints formulated from Lyapunov stability criteria at each vertex.

3 Robust Control Design

The fundamental of the cruise control problem is speed tracking performance, thus in this section, robust control design based on the H-infinity approach is presented, which is able to handle the uncertainties and the disturbances of the system. The problem formulation of the objectives of this paper is listed as follows:

1. To reduce the speed tracking error with respect to a set reference speed in order to have comfortable driving performances.
2. To ensure that the driving/braking control signal is always achievable by the control actuator.
3. To enhance overall system performances in traffic flow.

From the state representation in (8), the performance of the system is the tracking of the reference speed set by driver and the minimization of the control input, which are described as

follows:

I. Acceptable tracking error, to reduce the journey time requirement such that the performance of the vehicle is as in (11):

$$z_1 = |v_{ref} - v| \rightarrow min \quad (11)$$

II. Minimal control input, to reduce fuel consumptions. such that the performance of the vehicle is as follows:

$$z_2 = |u| \rightarrow min \quad (12)$$

Finally, the closed loop interconnection structure together with the weighting functions are shown in fig 1. Now, to get the generalized plant P for the mixed sensitivity H-infinity control problem, we defined the variables as follows:

$w(t) = [v_{ref}(t),\ d(\theta)]$ are the exogenous input signals
$u(t) = [F_x(t)]$ are the control inputs signal
$y(t) = (v_{ref} - v)$ is the signal measurement output
$z(t) = [z_1(t), z_2(t)]$ are the controlled output signals.

The general state-space representation of the plant is formulated as:

$$P: \begin{cases} \dot{x(t)} = A(\rho)x + B_1 w(t) + B_2 u(t) \\ z(t) = C_1 x + D_{12} u(t) \\ y(t) = C_2 x \end{cases} \quad (13)$$

To scale the signals of the system, the approach in [3] was adopted as follows; to characterize the performance specification and actuator frequency limitations:

- z_1, speed error control output signal, is the output of the tracking error performance weight defined:

$$w_e = \left(\frac{S/M_s + 2\pi f_c}{S + 2\pi f_c \in}\right) \quad (14)$$

Where $M_s = 2$ is the maximum peak magnitude, $f_c =$ 0.23Hz is the cut-off frequency of a high-pass filter (i.e. Settling time of 6s), $\in$= 0.001 is the attenuation level for low frequencies yield (i.e. tracking error ≤ 0.1%).

- z_2, the driving force control signal attenuation, is the output of the control Actuator performance weight defined as:

$$w_u = 1/f_{max} \quad (15)$$

Where $F_{,max}$= 6KN is the maximum limit of the drive/brake actuator intervention. This filter is designed in order to limit the driving force of vehicle with nominal mass of 1800kg moving on max of 30% road grade. Thus, the interest of such filter is to avoid saturation of actuator.

- $d(\theta)$, the exogenous disturbance input signal, due to road inclination and rolling resistance, with performance weight defined as:

$$w_d = Crgcos\theta + gsin\theta \quad (16)$$

Where $w_d = 5$ is the Maximum disturbance attenuation due to road condition and the tire resistance. This is also designed to limit the disturbance of vehicle moving at high speed on max of 30% road grade.

Remark: the robustness of the system requires the consideration of the highest bound of w_u from maximum τ value in the control design. This maximum τ is related to the slowest actuation of the driveline/braking systems.

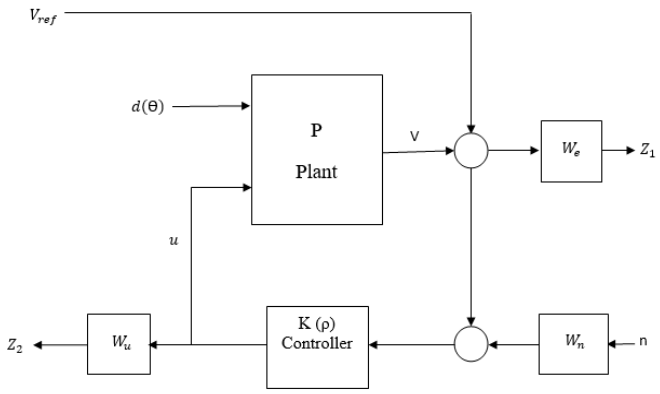

Fig. 1. closed-loop interconnected control structure

Now, the control objective is to find a stable dynamical output feedback controller K(ρ), so that for a given real value of γ and by using L_2 norm, the H-infinity norm of the closed loop system yield:

$$sup(\|z\|_2/\|w\|_2) \leq \gamma \quad (17)$$

From the generalize plant (13), All sufficient conditions to apply polytopic approach were met, thus we can find a stabilized polytopic LPV controller with a finite dimension, ensuring H-infinity performances of (17), the following proposition has to be satisfied.

Proposition 1. *Feasibility – H-infinity LMI based design [6] Solving the following LMIs in ($\mathbf{X}$, $\mathbf{Y}$, $\widetilde{\boldsymbol{A}}(\rho_1, \rho_2)$, $\widetilde{\boldsymbol{B}}$, $\widetilde{\boldsymbol{C}}and\widetilde{\boldsymbol{D}}$) at each vertices of the polytope while minimizing γ.*

$$\gamma^* = min\,\gamma \quad (18)$$

$$s.t\ (19) I_{(\rho_{1min}, \rho_{2min})}$$
$$s.t\ (19) I_{(\rho_{1min}, \rho_{2max})}$$
$$s.t\ (19) I_{(\rho_{1max}, \rho_{2min})}$$
$$s.t\ (19) I_{(\rho_{1max}, \rho_{2max})}$$

$$\begin{bmatrix} P_{11} & (*)^T & (*)^T & (*)^T \\ P_{21} & P_{22} & (*)^T & (*)^T \\ P_{31} & P_{32} & -\gamma \mathrm{I} & (*)^T \\ P_{41} & P_{42} & P_{43} & -\gamma \mathrm{I} \end{bmatrix} < 0, \begin{bmatrix} \mathbf{X} & I_n \\ I_n & \mathbf{Y} \end{bmatrix} > 0 \quad (19)$$

Where :

$$P_{11} = A(\rho_1, \rho_2)\mathbf{X} + \mathbf{X}A^T(\rho_1, \rho_2) + B_2\widetilde{\boldsymbol{C}} + \widetilde{\boldsymbol{C}}^T \mathrm{B}_2{}^{\mathrm{T}}$$
$$P_{21} = \widetilde{\boldsymbol{A}}(\rho_1, \rho_2) + A^T(\rho_1, \rho_2) + C_2{}^{\mathrm{T}}\widetilde{\boldsymbol{D}}^T \mathrm{B}_2{}^{\mathrm{T}}$$
$$P_{22} = \mathbf{Y}A(\rho_1, \rho_2) + A^T(\rho_1, \rho_2)\mathbf{Y} + \widetilde{\boldsymbol{B}}C_2 + C_2{}^{\mathrm{T}}\widetilde{\boldsymbol{B}}^{\mathrm{T}}$$
$$P_{31} = B_1{}^{\mathrm{T}} + D_{21}{}^T\widetilde{\boldsymbol{D}}^T B_2{}^T$$
$$P_{32} = B_1{}^{\mathrm{T}}Y + D_{21}{}^T\widetilde{\boldsymbol{B}}^T$$
$$P_{41} = \mathrm{C}_1\mathbf{X} + D_{12}\widetilde{\boldsymbol{C}}$$

$P_{42} = \mathrm{C}_1 + D_{12}\widetilde{\boldsymbol{D}}C_2$
$P_{43} = \mathrm{D}_{11} + D_{12}\widetilde{\boldsymbol{D}}D_{21}$

Proposition 2. *Reconstruction [6] - If proposition 1 is satisfied, then the controller K(ρ) exist, then the reconstructed controller is obtained solving the following system of equation at each vertex using the following equivalent transformation to solve – H-infinity LMI based.*

$$(21)I_{(\rho_{1min},\rho_{2min})}$$
$$(21)I_{(\rho_{1min},\rho_{2max})}$$
$$(21)I_{(\rho_{1max},\rho_{2min})}$$
$$(21)I_{(\rho_{1max},\rho_{2max})} \quad (20)$$

$$A_k(\rho) = N^{-1}(\widetilde{\boldsymbol{A}}(\rho_1,\rho_2) - \widetilde{\boldsymbol{YA}}(\rho_1,\rho_2)\boldsymbol{X} - \boldsymbol{Y}B_2D_CC_2\boldsymbol{X} - NB_CC_2\boldsymbol{X} - \boldsymbol{Y}B_2C_CM^T)M^{-T}$$
$$B_k = N^{-1}(\widetilde{\boldsymbol{B}} - \boldsymbol{Y}B_2D_C)$$
$$C_k = (\widetilde{\boldsymbol{C}} - D_CC_2\boldsymbol{X})M^{-T} \quad (21)$$

Where, M and N are defined such that $MN^T = I - XY$ (that can be solved through a singular value decomposition plus a Cholesky factorization).
Thus, the dynamical output feedback polytopic LPV controller will have the form. $K(\rho) = \begin{bmatrix} A_k(\rho) & B_k \\ C_k & D_k \end{bmatrix}$.

Remarks: See the work of [7],[8],[9],[10] for further details of proofs and numerical issues to improve matrix condition.
As long as the polytopic design has been used for synthesis, the LPV polytopic controller can be realized as follows:

- Obtaining Linear Time Invariant (LTI) controller at each vertex of the polytope by solving the LPV/H-infinity problem for the upper and lower bounds of the varying parameters.
- Then, formulate the global LPV controller ensuring the system stability is a convex combination of the previously obtained controllers at each vertex.

Which can be mathematically described as follows:
$K(\rho) = \alpha_1 K(\rho_{1min},\rho_{2min}) + \alpha_2 K(\rho_{1min},\rho_{2max}) + \alpha_3 K(\rho_{1max},\rho_{2min}) + \alpha_4 K(\rho_{1max},\rho_{2max})$ (22)

Where the scheduling variables are as follows:

$$\alpha_1 = \frac{(\rho_{1max}-\rho_1)(\rho_{2max}-\rho_2)}{(\rho_{1max}-\rho_{1min})(\rho_{2max}-\rho_{2min})}$$

$$\alpha_2 = \frac{(\rho_{1max}-\rho_1)(\rho_2-\rho_{2min})}{(\rho_{1max}-\rho_{1min})(\rho_{2max}-\rho_{2min})}$$

$$\alpha_3 = \frac{(\rho_1-\rho_{1min})(\rho_{2max}-\rho_2)}{(\rho_{1max}-\rho_{1min})(\rho_{2max}-\rho_{2min})}$$

$$\alpha_4 = \frac{(\rho_1-\rho_{1min})(\rho_2-\rho_{2min})}{(\rho_{1max}-\rho_{1min})(\rho_{2max}-\rho_{2min})}$$

4 Result And Discussion

4.1 Synthesis Result

By applying Propositions 1 and 2 above, for $\{\rho_1,\rho_2\} = [\rho_{1min},\rho_{1max}] \times [\rho_{2min},\rho_{2max}]$, with YALMIP parser [9] and SeDuMi solver [10], the following sensitivity functions are obtained in fig .2 and fig .3 for the polytopic LPV problems with minimum attenuation ($\gamma* = 1.827$).

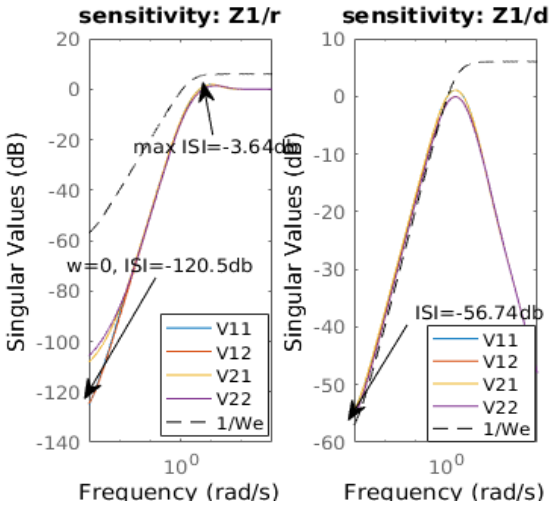

Fig.1. z_1 controlled output of the 4 vertices LTI (a/left-response to reference, b/right-response to disturbance)

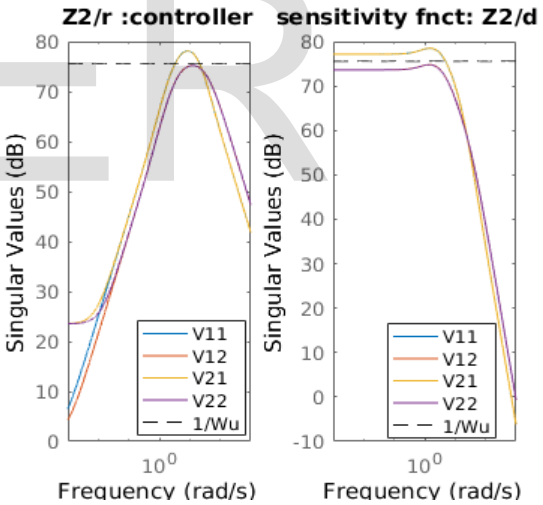

Fig. 2. z_2 controlled output of the 4 vertices LTI (a/left-response to reference, b/right-response to disturbance)

Performance and robustness Analysis

The speed of a vehicle is viewed as a constant reference signal; thus, low frequency will be our region of interest, such that $\omega_s < \omega_c < \omega_T$.

Z_1/r: Fig .2-a shows the response of the speed error to reference speed, the system meets the trade-off of the desired templates i.e. At low frequency, $|\ \mathbf{Z_1/r}(j\omega)\ |$ is also low with a steady state error in of approximately **–120db** at $w \approx 0\,rad/s$. Moreover, the peak value of max $|\ \mathbf{Z_1/r}(j\omega)\ |$ is less than the module margin of robustness (i.e. $M_s \leq$ -6db). Thus, a small speed error is guaranteed for low frequencies and speed error

is well attenuated even at maximum peak frequency.

Z_1/d: Fig .2-b gives the response of the speed error to tire and inclination resistance, because disturbances typically are of low frequencies, the system meet the trade-off i.e. $|\mathbf{Z_1/d}(j\omega)|$ is low at low frequencies. Furthermore, at $w \approx 0\,rad/s$, $|SG(j\omega)|$=0. Thus, robustness of the speed error due to disturbances is well guaranteed with maximum attenuation.

Z_2/r: Fig .3-a gives the response of the driving force to reference speed. The control acts on the specified frequency range as a bandwidth filter below the maximum set limit, in order to avoid saturation of output due to excessive reference speed. One can said, the system meets the trade-off with actuator constraint i.e. $|\mathbf{Z_2/r}(j\omega)|$ is lower than the maximum set limit at high frequencies. Thus, preserving the drive/brake actuator saturation.

Z_2/d: Fig .3-b gives the response of the driving force to noise injected by tire and inclination resistance. because noise signals typically are of high frequencies, then one can say the system meet the trade-off of the desired template i.e. $|\mathbf{Z_2/d}(j\omega)|$ is low at high frequencies. Consequently, the actuator is well preserved from high frequencies signals due to tire and inclination.

4.2 Simulation Results

In this section, simulations scenario with different kinds of driving situation is performed to illustrate the benefit of the control design and to show that the controller output signals fulfil the speed regulation, which is the main contributions of this paper.

Remark: For performance comparison purpose, the LPV controlleris benchmarked with respect to a Nominal LTI controller form.$K_{nominal} = \begin{bmatrix} A_{kn} & B_{kn} \\ C_{kn} & D_{kn} \end{bmatrix}$

4.2.1 First Simulation - flat road "d=0"

From control theory, the LPV controller is proved to have better performance and robustness than LTI controller counterpart in [6]. In simulation, a small vehicle with nominal mass of 1200kg and the maximum gross mass with the passengers and luggage of 1800kg, moving at different speeds is tested on a reference complex nonlinear vehicle model.

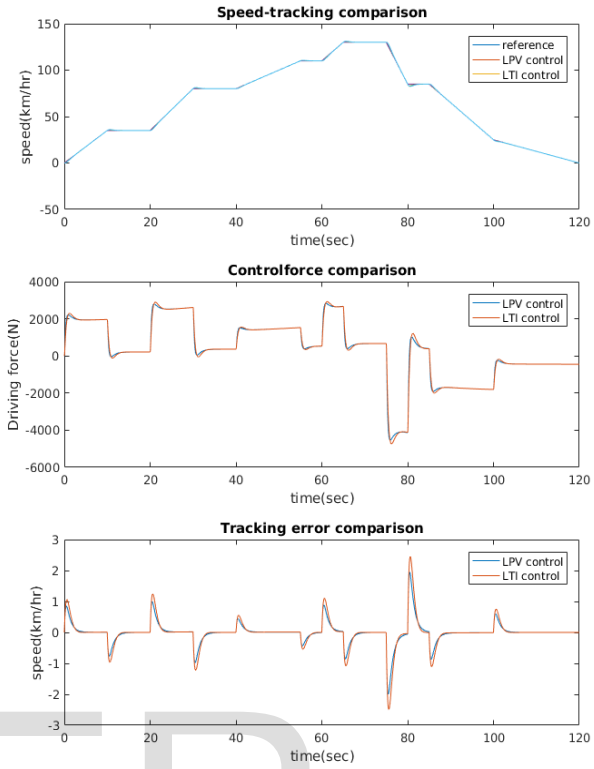

Fig.3 Simulation result-performance comparison (Blue- -LPV response, red-LTI response), '**d =0**'

Performance analysis

Although both the control responses of the system on a flat road (i.e. d ≈ 0) show sufficient performance in fig .4, but the LPV has faster response than it LTI counterpart. when the car is moving at maximum acceleration of **1.25m/s²** at **20s**, LPV and LTI speed errors are 1km/hr and 1.2km/hr respectively (i.e. difference of 0.2km/hr) with a common driving force of approximately 2.5KN. Whereas, when there is instant braking with **2.78m/s²** at **70s**, the LPV and LTI speed errors are 2km/hr and 2.5km/hr respectively (i.e. difference of 0.5km/hr) with a common braking force of 4KN. In addition, the speed error is same for both controllers when the vehicle is speeding uniformly. Therefore, we can conclude the propose control strategy is effective and the LPV controller is once more proved to be better than LTI counterpart and proposed e-MPC controller of reference in [5].

Robustness analysis

In order to verified the robustness of the system obtained from frequency response result, its good we show the time domain analysis which is more conversant to all type of analyzers. We simulate a **30%** loss of control due to uncertainties at **60s**. Fig .5 shows result obtained, there exists a negligible difference in the speed tracking error and driving force compared to normal operation of the system. For instance, the tracking

error is still 1km/hr at 60s and 2km/hr at 80s in both normal- fig .4 and abnormal- fig .5 situation. Hence, the system is indeed robust to loss in control due to uncertainties.

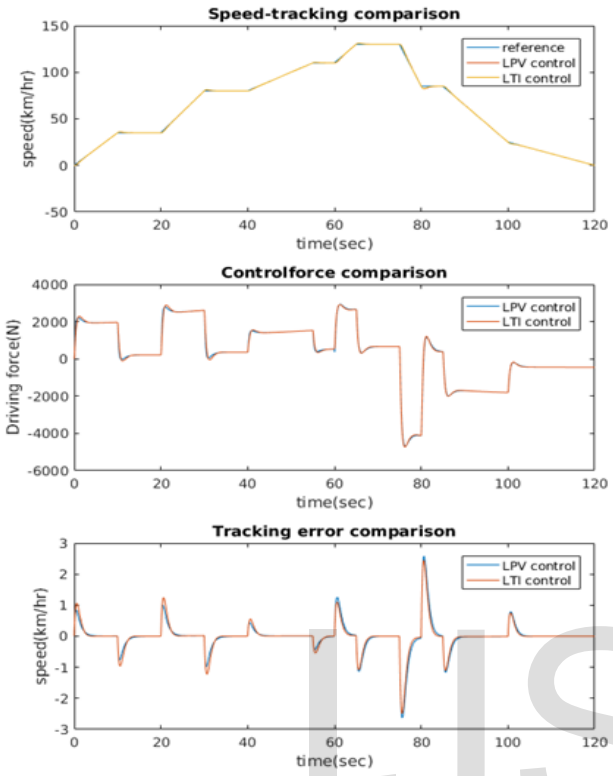

Fig. 4 Simulation result-loss of control (Blue- -LPV response, red-LTI response), '**d =0'**

4.2.2 Second simulation – inclined road "d >0"

Road inclination is a very important factor to be considered in speed profile control. Assuming the same speed profile scenario used in (4.2.1) above is repeated with variation in road slope (%) assumed to be estimated by sensor such as GPS, radar.

To investigate the effect of different road inclination on the proposed control strategy, we generate a disturbance signal with varying road slope (%) due to tire and road inclination resistance.

Remark: According to AASHTO highway subcommittee on design, the maximum grade of a road is 25%, usually the road gradient of most highway doesn't exceed 5% and on local road it could reach 15%, but normally it should be taken 20% for design.

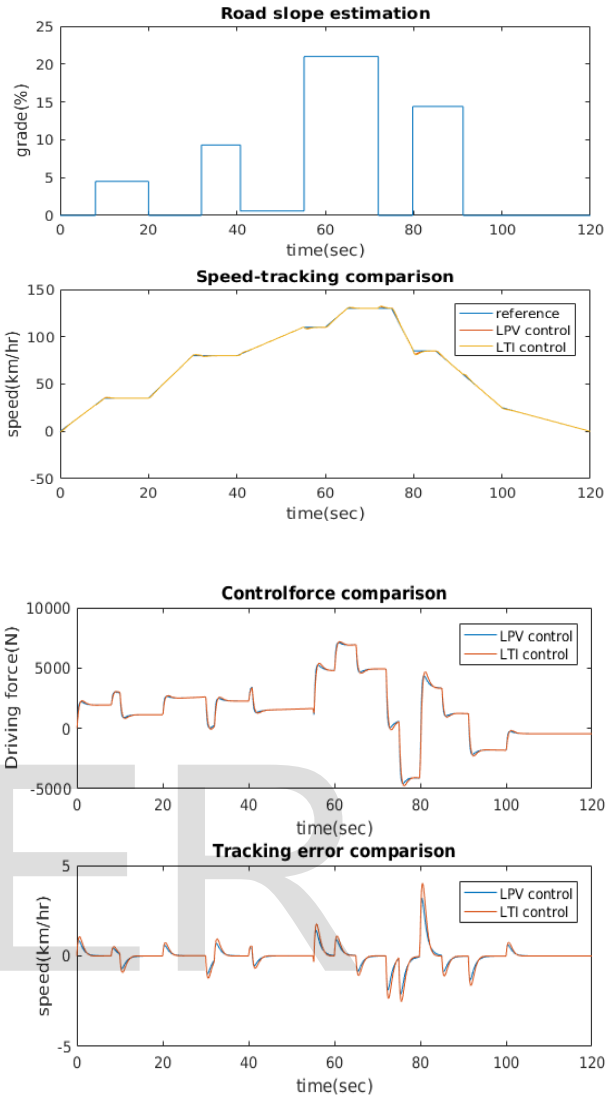

Fig. 5 Simulation result-performance comparison (Blue- -LPV response, red-LTI response), '**d >0'**

Performance Analysis:

Comparing results obtained in this case with the previous one with constant slope, the disturbance rejection behavior of the control system is acceptable and the vehicle's speed is slightly decreased in the presence of the road grade resistance torque in fig .6, we can see that both speed tracking error and driving force are still robust to ascending change in road slope while accelerating between **0-60s**,but when the ascending road slope is more than **20**% grade at **60-70s**, enormous driving force is required around 7KN which is almost 300% of the normal driving force with a minor noticeable variations in the speed tracking error. Furthermore, when there is an instant braking at **75s** on descending road slope, the braking force is huge enough to cause very large speed tracking error of 3.8km/hr. Thus, despite significant effect of the road slope on the driving force requirement and speed tracking performance, the proposed control scheme is robust to acceptable variation of road conditions-

4 CONCLUSION

In this paper, the overall objective was to designed an efficient LPV controller for ACC strategies. The task of this control is to improve the longitudinal automation of the vehicle, which include speed tracking performance, traffic through-put, safety and ride comfort, energy saving.

Lyapunov stability criteria was used to ensure the global stability of the system within the set of operating conditions, which was validated from the exponential converges of system response, and also signify an excellent trade-off between tracking accuracy and ride comfort.

To confirm our results, performance comparison of the designed LPV ACC strategy with the LTI counter-part and other ACC strategies used in literature is done, which shows significant improvement and guaranty robustness against uncertainties. In addition, eliminating the input disturbance in the controller design may render the system performance and robustness when subjected to large scale of disturbances

To conclude, formulation of stable q-LPV longitudinal model of vehicle was successfully achieved and used to designed a polytopic LPVH-infinity controller. Thus, improvement of the speed tracking performance and robustness in mass and road variation, with minimum driving force was achieved while maintaining ride comfort, these indeed reduce journey time and energy consumption.

REFERENCES

[1] On-Road Automated Vehicle Standards Committee. "Taxonomy and definitions for terms related to on-road motor vehicle automated driving systems". *SAE International*, 2014. (URL link https://www.sae.org/standards/content/j3016_201401/)

[2] Gaspar, Peter, and Balazs Nemeth. "Design of Look-Ahead Control for Road Vehicles Using Traffic Information." *22nd Mediterranean Conference on Control and Automation, IEEE*, pp. 201–06. 2014. (Conference preceding)

[3] Nemeth, Balazs, and Peter Gaspar. "Model-Based Sensitivity Analysis of the Look-Ahead Cruise Control." *15th International Symposium on Computational Intelligence and Informatics (CINTI), IEEE*, pp. 103–08. 2014. (Conference preceding)

[4] Németh, Balázs, and PéterGáspár. "Robust Look-Ahead Cruise Control Design Based on the $\mathcal{H}\infty$ Method∗∗This Paper Was Supported by the JánosBolyai Research Scholarship of the Hungarian Academy of Sciences." *IFAC-Papers OnLine*, vol. 48, no. 14, pp. 19–24. 2015 (Journal citation)

[5] Németh, B., Gáspár, P., Orjuela, R., & Basset, M. "LPV-Based Control Design of an Adaptive Cruise Control System for Road Vehicles." *IFAC-Papers OnLine*, vol. 48, no. 14, pp. 62–67, 2015. (Journal citation)

[6] Seshia S. A., Sadigh D., & Sastry S. S. "Formal Methods for Semi-Autonomous Driving." *Proceedings of the 52nd Annual Design Automation Conference on - DAC '15, ACM Press*, pp. 1–5, 2015. (Conference preceding)

[7] Poussot-Vassal C., Sename O., Dugard L., & Savaresi S. M "Vehicle Dynamic Stability Improvements through Gain-Scheduled Steering and Braking Control." *Vehicle System Dynamics*, vol. 49, no. 10, pp. 1597–621. Oct. 2011. (Journal citation)

[8] Scherer C., Gahinet, P., & Chilali, M. "Multiobjective Output-Feedback Control via LMI Optimization." *IEEE Transactions on Automatic Control*, vol. 42, no. 7, pp. 896–911, July 1997. (IEEE transaction)

[9] Gahinet, P., Apkarian, P., & Chilali, M. "Affine Parameter-Dependent Lyapunov Functions and Real Parametric Uncertainty." *IEEE Transactions on Automatic Control*, vol. 41, no. 3, pp. 436–42, Mar. 1996. (IEEE transaction)

[10] Lofberg, J. "YALMIP : A Toolbox for Modeling and Optimization in MATLAB." *IEEE International Conference on Robotics and Automation (IEEE Cat. No.04CH37508), IEEE*, pp. 284–89, 2004. (Conference preceding)

[11] Sturm, Jos F. "Using SeDuMi 1.02, A Matlab Toolbox for Optimization over Symmetric Cones." *Optimization Methods and Software*, vol. 11, no. 1–4, pp. 625–53, Jan. 1999. (Conference preceding)